Available online at www.sciencedirect.com
SCIENCE DIRECT®
Journal of Nuclear Materials 337–339 (2005) 456–460
journal of nuclear materials
www.elsevier.com/locate/jnucmat

Development of ICRF wall conditioning technique on divertor-type tokamaks ASDEX Upgrade and JET

A. Lyssoivan [a,*], D.A. Hartmann [b], J.-M. Noterdaeme [b,c], R. Koch [a], V. Bobkov [b], T. Blackman [d], F. Braun [b], M. Cox [d], P. de Vries [d], H.G. Esser [e], H.-U. Fahrbach [b], J. Gafert [b], E. Gauthier [f], O. Gehre [b], M. Graham [d], G. Haas [b], A. Huber [e], K. Lawson [d], P.J. Lomas [d], M. Mantsinen [g], G. Matthews [d], M.-L. Mayoral [d], A. Meigs [d], Ph. Mertens [e], V. Mertens [b], I. Monakhov [d], J. Neuhauser [b], V. Philipps [e], V. Rohde [b], M. Santala [g], W. Suttrop [b], A. Walden [d], D. Van Eester [a], F. Wesner [b], ASDEX Upgrade Team and JET EFDA Contributors

[a] *Association EURATOM-BELGIAN STATE, LPP-ERM/KMS, 30 Avenue de la Renaissance, 1000 Brussels, Belgium* [1]
[b] *EURATOM Association, Max-Planck Institut für Plasmaphysik, D-85748 Garching, Germany*
[c] *EESA Department, Gent University, B-9000 Gent, Belgium*
[d] *Association EURATOM-UKAEA, Culham Science Centre, Abingdon OX14 3DB, UK*
[e] *EURATOM Association, Institut für Plasmaphysik FZ Jülich, D-52425 Jülich, Germany* [1]
[f] *Association EURATOM-CEA, DSM-DRFC, CEA Cadarache, 13108 St. Paul lez Durance, France*
[g] *Association EURATOM-TEKES, Helsinki University of Technology, FIN-02015 HUT, Finland*

Abstract

Encouraging results of efficient wall conditioning with ICRF discharges achieved on the circular tokamaks (without divertors) TEXTOR, TORE SUPRA, HT-7 stimulated the next step in the development of an alternative wall conditioning technique that is relevant to reactor-scale superconducting fusion machines. Here, the first results on the ICRF discharge initiation and the wall conditioning on the large-size non-circular tokamaks ASDEX Upgrade and JET using the standard ICRF antennas are reported. Analysis of the mass-spectrum data on both machines indicates noticeable outgassing of deuterium, water and hydrocarbons from the walls despite operating with a non-optimized set of ICRF discharge parameters.
© 2004 Elsevier B.V. All rights reserved.

PACS: 52.40.Hf; 52.50.−b; 52.55.Fa; 52.80.Pi
Keywords: ITER; Wall conditioning; ICRF antenna; RF discharge

1. Introduction

In future reactor-scale *superconducting* fusion devices such as ITER, the presence of permanent high magnetic

* Corresponding author. Tel.: +49 2461 61 6473; fax: +49 2461 61 3331.
E-mail address: a.lyssoivan@fz-juelich.de (A. Lyssoivan).
[1] Partners in the Trilateral Euregio Cluster (TEC).

0022-3115/$ - see front matter © 2004 Elsevier B.V. All rights reserved.
doi:10.1016/j.jnucmat.2004.07.060

field will prevent the use of conventional *Glow Discharge Conditioning* (G-DC) in between shots due to short-circuit occurring between anode and cathode along the magnetic field lines. The need of controlled and reproducible plasma start-up and tritium removal, e.g. from the co-deposited carbon layers, will require applying an *alternative* wall conditioning procedure in future fusion machines. Conditioning by RF discharges generated with waves in the ion cyclotron range of frequencies (ICRF-DC) is fully compatible with the presence of a magnetic field. ICRF-DC has been developed on the circular tokamaks (without divertors) TEXTOR [1,2], TORE SUPRA [3,4] and HT-7 [5] using the present generation ICRF antennas without any modifications in hardware.

The conditioning efficiency, evaluated in terms of the rate of hydrogen removal during operation of the conditioning plasmas, was found to be much higher for ICRF-DC than for G-DC (about 10–20 times higher, TORE SUPRA [3], HT-7 [5]) or for ECRF-DC performed with a focused microwave beam (about 25 times higher, TEXTOR [2]). Principles of ICRF plasma production were formulated in Ref. [6]. Analysis showed that ICRF-DC could be extrapolated to ITER [6].

The encouraging efficiency of wall conditioning achieved with ICRF-DC on circular tokamaks stimulated the next step in the development of this alternative wall conditioning technique that is relevant to reactor-scale superconducting fusion machines. We report the first results obtained on the ICRF discharge initiation and the wall conditioning on the large-size non-circular tokamaks ASDEX Upgrade (AUG) and JET.

2. Experimental set-up

The experiments on both machines have been performed using the standard ICRF systems and under the following conditions:

- On AUG (plasma major radius $R_0 = 1.65$ m, horizontal $a_h \approx 0.5$ m and vertical $a_v \approx 0.8$ m minor radii): 1 to 4 ICRF antennas (each consists of two poloidal current straps) [7] were used with $P_{RF/ant} \approx 3$–120 kW, $f = 30$ MHz and π-phasing. The ICRF system operated without any modifications in hardware. Multi-pulse (6×300 ms) or long pulse (up to 4 s) operations were performed with a magnetic field $B_T = 1$–2 T in helium in the pressure range $p_{He} = (1–8) \times 10^{-2}$ Pa. The regime of continuous helium flow with feedback control was chosen in the experiment.
- On JET ($R_0 = 2.96$ m, $a_h \approx 1.25$ m, $a_v \approx 2.10$ m): one ICRF antenna (array C with four poloidal current straps) [8] was used with $P_{RF\text{-}tot} \approx 130$–245 kW, $f \approx 34$ MHz, π-phasing and pulse length $\tau_{RF} = 0.5$–4 s. Some modifications in the RF generator control system were done to manage operation in the RF plasma generation regime. The machine operated at $B_T = 1.85$–2.45 T in helium or in a mixture of helium and hydrogen (80% He, 20% H_2 gas puffing mode without feedback control). Due to technical constraints (pressure trip level of the antenna vacuum transmission line (VTL) is $\sim 1 \times 10^{-2}$ Pa), experiments on JET were performed at lower gas pressure in the torus, $p_{tot} \approx (1–8) \times 10^{-3}$ Pa.

3. Results and discussion

3.1. Neutral gas ICRF breakdown

To develop a reliable wall conditioning technique, efficient for large-size fusion machines, special emphasis was given to study the physics of ICRF discharges. This type of RF discharge evolves from the neutral gas local breakdown due to initial electron impact ionization by the antenna-near field $\widetilde{E}_z$ (parallel to the B_T-field and evanescent in vacuum) to the main phase of plasma production over the torus due to plasma waves propagation ($\omega < \omega_{pe}$) and absorption mainly by electrons resulting in further volume ionization [6]. A 3-D electromagnetic modeling of the present-day ICRF antennas with and without Faraday shields showed that the antennas can generate in vacuum the $\widetilde{E}_z$-field of the amplitude necessary for neutral gas breakdown and plasma production [6]. However, the first (gas breakdown) phase of the ICRF discharge is considered as the most critical one with respect to the antenna RF voltage and loading due to the fast transition from vacuum to plasma conditions. To avoid deleterious effects of the neutral gas breakdown and arcing inside the antenna box at this phase, the frequency of RF generators and the RF voltage/power at antenna straps were reduced to technically available minimal values still meeting the requirements for ICRF breakdown [6]:

$$(\omega/e)(2m_e\varepsilon_i)^{1/2} \leqslant \widetilde{E}_z(r) \leqslant m_e\omega^2 L_z/(2e). \quad (1)$$

Here ε_i is the ionization energy threshold, $L_z = 2\widetilde{E}_z/(\mathrm{d}\widetilde{E}_z/\mathrm{d}z)$ is the parallel length scale of the RF ponderomotive potential [6].

As a result of the precautionary measures, reliable RF breakdown of the neutral gas and discharge initiation ($\omega \approx 4\omega_{cHe+} = \omega_{cH}$) were possible in both machines over the whole parameter range covered. Fig. 1 shows the transition from the RF breakdown phase to the ICRF discharge phase in JET. Here $\langle P_{RF/strap} \rangle$ and $\langle V_{RF/strap} \rangle$ are the RF power and the RF voltage at antenna, both averaged over four radiating straps. It is

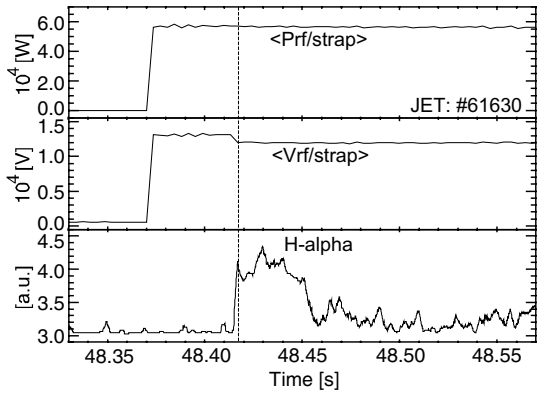

Fig. 1. The transition from the neutral gas breakdown phase to the ICRF discharge phase in JET.

clearly seen that the gas breakdown occurs after some delay and shows up in a drop in the antenna RF voltage and in a burst in the H_α emission (measured far away from the antenna port). From the point of view of ICRF system operation, such a correlation is the sign of RF discharge initiation *outside* of the antenna box and subsequent plasma propagation along the magnetic field lines. The pressure dependence of the neutral gas breakdown time (associated with the RF voltage drop and the occurrence of the initial peak in the H_α emission) is plotted in Fig. 2 for RF discharges with similar RF power per strap (30–50 kW) and frequency (~30 MHz). A tendency towards an increase in breakdown time at low pressure is clearly seen. This results from the reduced collisionality and probability for an ionization event. Data from three tokamaks (TEXTOR, AUG and JET) were found in a good agreement (Fig. 2), which might be an indication that the antenna RF voltage (the antenna-near $\widetilde{E}_z$ electric field) plays a fundamental role in the neutral gas ICRF breakdown and that the breakdown time is independent on the machine size. However, more data from JET are necessary for detailed analysis.

3.2. ICRF discharge/plasma characterization

Further analysis of the ICRF discharge phase revealed that the antenna–plasma coupling efficiency (fraction of generator power radiated into the plasma, $\eta = P_{\text{RF-pl}}/P_{\text{RF-tot}} = (R_{\text{ant-tot}} - R_{\text{ant-vac}})/R_{\text{ant-tot}}$) was between 50% (high B_T) and 75% (low B_T) at AUG. This result was found in agreement with the TEXTOR and TORE SUPRA data base [4,6] and in line with the fast wave propagation properties [4]. Unexpectedly low antenna coupling efficiency at JET (less than 25% according to a preliminary estimate) resulted in the antenna operation at RF voltages close to the upper limit and sporadic tripping occurred. This will be the subject of further investigations.

The CCD cameras monitoring RF discharges in toroidal and poloidal directions indicated that ICRF plasmas were toroidally uniform (like on circular machines) but poloidally located mostly at the machine low field side, LFS (ICRF antennas side). The ECE radiation temperature data confirmed that RF plasmas radially extended in front of the AUG ICRF antennas by 15 cm only. To improve the RF plasma homogeneity, several recipes have been used in the experiments. On AUG, the poloidal extent of the plasma could be increased by superposing an additional vertical magnetic field ($B_V \ll B_T$). On JET, the plasma extended radially over the vessel center towards the HFS when a gas mixture of helium and hydrogen (80% He, 20% H_2) was injected (Fig. 3). This had been predicted from the electron

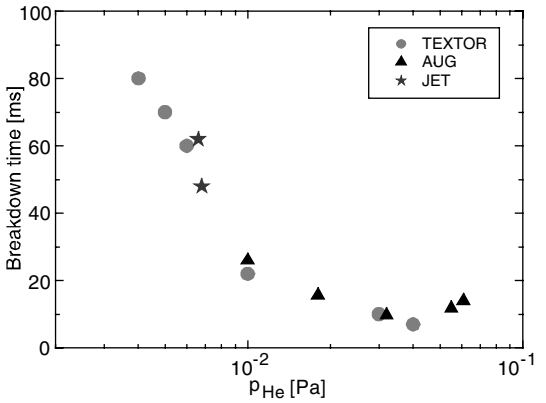

Fig. 2. Pressure dependence of the RF breakdown time derived from the H_α emission analysis (P_{RF}/antenna strap ≈ 30–50 kW, $f \approx 30$ MHz, $\omega = 4\omega_{cHe+} = 2\omega_{cD} = \omega_{cH}$).

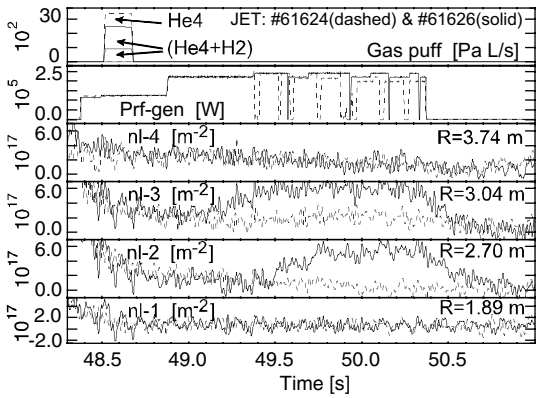

Fig. 3. Evolution of the line-integrated density for two similar ICRF discharges in JET performed in helium (#61624, dashed) and in a gas mixture of ~80% He and ~20% H_2 (#61626, solid).

power deposition profiles calculated with the 1D RF model of Ref. [9] for helium RF plasmas with variable H concentrations.

Analysis of the core atomic spectroscopy data showed appearance of the H_α, D_α and HeI (neutral) lines during the JET ICRF discharges. The impurity analysis of the VUV spectroscopy data indicated that the main impurity observed in JET ICRF discharges was HeI (dominated the spectrum) with the HeII line weak present and clear evidence of CII in the long pulse RF shot #61631 ($\tau_{RF} = 4$ s). Assuming an equilibrium (coronal) ionization balance, T_e can be approximately derived from the ionization stages observed. This evaluation resulted in $T_e \sim 2$–3 eV for shots at the gas pressure $p_{tot} \approx (4–6) \times 10^{-3}$ Pa and $T_e \sim 4$–5 eV when gas pressure decreased ($p_{tot} \approx 2 \times 10^{-3}$ Pa). *There was no evidence in the VUV spectrum of lines or bands of lines that could be due to metals.*

Analysis of the line-integrated density on both machines ($n_e l \leqslant 6 \times 10^{17}$ m^{-2}) showed that the RF plasma density was proportional to the injected RF power (a sign of weakly ionized plasma) and increased with the torus pressure. The ionization degree roughly estimated from the averaged density/pressure measurements was found to be rather low, $n_e/(n_e+n_0) < 0.1$.

On both tokamaks, high-energetic fluxes of H (with energies up to 60 keV) and of D atoms (up to 25 keV) were detected by a neutral particle analyzer (NPA). Fig. 4 shows typical H and D atoms spectra observed in two similar AUG ICRF discharges performed in different magnetic fields. The NPA viewing line passed roughly through plasma center and was oriented along the torus major radius in horizontal plane and vertically with 13° upwards with respect to the horizontal plane. At $B_T = 2.0$ T (on-axis resonances $\omega = \omega_{cH} = 2\omega_{cD}$), H and D atoms spectra have the same shape up to 14 keV (curves 1 and 3, respectively) with the similar averaged energy $\overline{E}_{\perp H} \approx \overline{E}_{\perp D} \approx 3.0$ keV. On the contrary, for $B_T = 1.0$ T (twice higher on-axis cyclotron harmonic resonances $\omega = 2\omega_{cH} = 4\omega_{cD}$) clear evidence of tail formations in distribution functions of H and D atoms was observed (curves 2 and 4, respectively) with higher averaged energy for hydrogen ($\overline{E}_{\perp H} \approx 5.0$ keV, $\overline{E}_{\perp D} \approx$ 2.5 keV). This fact may be understood in terms of RF quasilinear diffusion: cyclotron harmonic heating tends to accelerate more the faster particles with tail formation at higher energy than fundamental heating [10]. However, we remind that the AUG ICRF plasmas were created mainly at LFS. Therefore, a minor population of protons and deuterons might be involved in the on-axis ion cyclotron heating. The observed phenomenon will be a subject for further analysis. The observations of high-energy H and D atom fluxes in AUG and JET ICRF plasmas confirm similar results previously reported from other ICRF wall conditioning experiments [3,5,6].

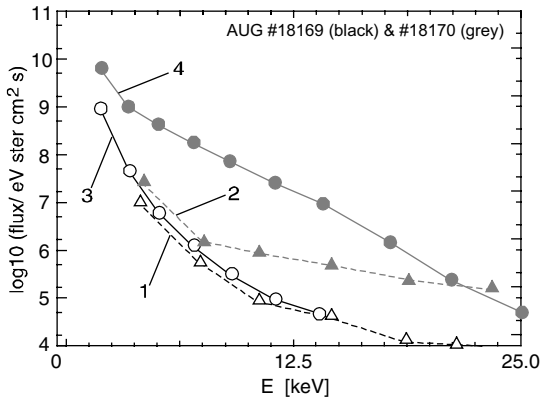

Fig. 4. Hydrogen (dashed lines 1, 2) and deuterium (solid lines 3, 4) atom spectra observed with NPA in the similar AUG ICRF discharges ($P_{RF} \approx 370$ kW, $p_{He} \approx 4.0 \times 10^{-2}$ Pa) at $B_T = 2.0$ T (black) and $B_T = 1.0$ T (grey).

3.3. ICRF discharge conditioning

The discharge conditioning is attributed to the removal of adsorbed gas species from the wall so that they may then be pumped out of the system. The adsorbed atoms may be removed by electronic excitation, chemical interaction and momentum/energy transfer [11]. For the latter mechanism, the rate of desorption increases with the impact energy of the ions and their masses [12]. ICRF discharges generate high-energetic fluxes of ions in a natural way due to presence of cyclotron mechanism (Fig. 4) and may be considered promising for wall conditioning.

The wall conditioning tests on both machines have been performed in the regime with single long RF pulse (4 s) operation. First analysis of the data of the residual gas analyzer (RGA) on AUG and JET yielded the following results. The wall conditioning effect could be seen by an increase in the partial pressure (outgassing) of H_2 HD, D_2 in the AUG case and similarly for masses $m = 2$, $m = 3$, $m = 4$, $m = 6$, $m = 18$, $m = 20$ in the JET case. The mass spectra of the residual gas recorded before and after the JET ICRF conditioning shot (#61631) were quite different (Fig. 5). The analysis of the fraction pattern revealed that the large increase in the mass-spectrum intensity for masses $m = 2$ (H_2 or D), $m = 3$ (HD) and $m = 4$ (D_2 or He) was probably due to both gas-into-vessel injection (80% He + 20% H_2 to initiate more homogeneous RF discharge) and gas release from the walls. Noticeable increase in the intensity for the other masses like $m = 6$ (D_3), $m = 18$ (CD_3, DO, H_2O), $m = 20$ (CD_4, D_2O), etc. may be attributed to the wall conditioning effect. However, more systematic studies are necessary to quantify more the wall release and conditioning effect.

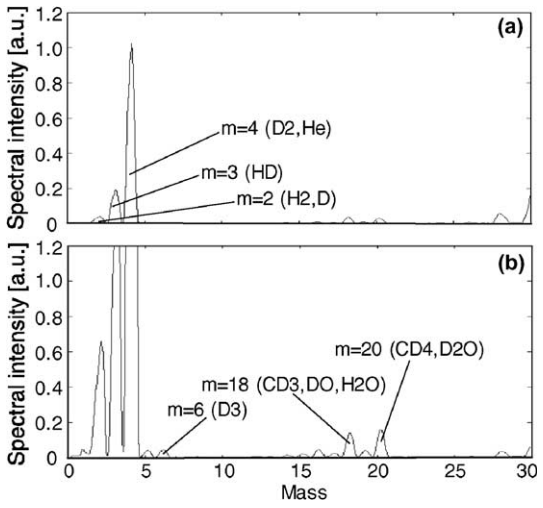

Fig. 5. Mass-spectrum of the residual gas in the JET vessel before (a) and after (b) the ICRF conditioning shot #61631 (constant $P_{\text{RF-gen}} \approx 230$ kW, decayed $B_{\text{T}} = 2.45$–1.85 T and $p_{\text{tot}} \approx (7\text{–}1) \times 10^{-3}$ Pa).

Acknowledgment

This work has been performed under the European Fusion Development Agreement. The authors gratefully thank Professor R. Weynants, Dr J. Paméla and Dr O. Gruber for their encouragement and stimulating support.

References

[1] H.G. Esser et al., J. Nucl. Mater. 241–243 (1997) 861.
[2] A. Lyssoivan et al., in: 14th Topical Conf. on Radio Frequency Power in Plasmas, Oxnard 2001, AIP Conf. Proceedings 595, New York, 2001, p. 146.
[3] E. de la Cal, E. Gauthier, Plasma Phys. Control. Fusion 39 (1997) 1083.
[4] A. Lyssoivan et al., in: 26th EPS Conf. on Control. Fusion and Plasma Phys., Maastricht, 1999, ECA, vol. 23J, 1999, p. 737.
[5] J.K. Xie et al., J. Nucl. Mater. 290–293 (2001) 1155.
[6] A. Lyssoivan et al., Final Report on ITER Design Task D350.2, Report LPP-ERM/KMS, 114, 1998.
[7] J.-M. Noterdaeme et al., Fusion Eng. Des. 24 (1994) 65.
[8] A. Kaye et al., Fusion Eng. Des. 24 (1994) 1.
[9] D. Van Eester, R. Koch, Plasma Phys. Control. Fusion 40 (1998) 1949.
[10] R. Koch, Trans. Fusion Sci. Technol. 45 (2004) 203.
[11] P.C. Stangeby, G.M. McCracken, Nucl. Fusion 30 (1990) 1225.
[12] J. Winter, Plasma Phys. Control. Fusion 38 (1996) 1503.